

EFFECT OF NANO ZIRCONIUM OXIDE (ZrO₂) PARTICLES ADDITION ON THE MECHANICAL BEHAVIOUR AND TENSILE FRACTOGRAPHY OF COPPER-TIN (Cu-Sn) ALLOY NANO COMPOSITES

UTICAJ DODATKA NANOČESTICA CIRKONIJUM OKSIDA (ZrO₂) NA MEHANIČKE OSOBINE I FRAKTOGRAFIJU PRI ZATEZANJU BAKAR-KALAJ (Cu-Sn) LEGURA NANOKOMPOZITA

Originalni naučni rad / Original scientific paper
UDK /UDC:

Rad primljen / Paper received: 28.09.2021

Adresa autora / Author's address:

¹) VTU RRC, Belgaum; Dept. of Mechanical Engineering, Oxford College of Engineering, Bangalore, Karnataka, India *email: madev.nagaral@gmail.com

²) Dept. of Mechanical Engineering, SJBIT, Bangalore, Karnataka, India

³) Dept. of Mechanical Engineering, Ramaiah Institute of Technology, Bangalore, Karnataka, India

⁴) Deputy Manager, Aircraft Research and Design Centre, HAL, Bangalore, Karnataka, India

⁵) Dept. of Mechanical Engineering, Oxford College of Engineering, Bangalore, Karnataka, India

⁶) Dept. of Mechanical Engineering, Siddaganga Institute of Technology, Tumkur, Karnataka, India

Keywords

- Cu-Sn alloy
- ZrO₂ nano particles
- stir process
- hardness
- tensile properties
- fractography

Abstract

In the current investigation, an exertion is prepared to produce copper-10%tin-nano ZrO₂ composites by exploiting melt technique. 4, 8, and 12 wt.% of nano ZrO₂ particles are introduced to the copper-tin (Cu-Sn) base network. Microstructural studies are performed by SEM, EDS, and XRD examination. Mechanical portrayal of Cu-10%Sn-4, 8, 12 wt.% of nano ZrO₂ composites are measured conferring to ASTM norms. Scanning electron micrographs uncovered the uniform conveyance of nano ZrO₂ in the copper-tin amalgam framework. EDX investigation affirmed the presence of Zr and O in nano-ZrO₂ built-up composites, and XRD designs uncovered the Cu, Sn, and ZrO₂ phases. It is further noticed that hardness, yield strength of Cu-Sn compound increased with the content of 4, 8, and 12 wt.% of nano-ZrO₂. Elongation of nano composites diminishes by adding oxide particles. Fractography of tensile examples is completed by utilising SEM micrographs to comprehend the failure of components.

INTRODUCTION

Metal composites are a unique combination of material system claiming their stake in numerous engineering applications. Some of their applications include automobile, aerospace, and biomedical components with domain specific relevance /1, 2/. Metal matrix composites have tailor made combinations of properties that include greater strength, higher stiffness, resistance to corrosion and wear, superior damping characteristics, low coefficient of thermal expansion, so on and so forth, /3, 4/.

Ključne reči

- legura Cu-Sn
- ZrO₂ nanočestice
- postupak mešanja
- tvrdoća
- zatezne osobine
- fraktografija

Izvod

U ovom istraživanju je izvedena priprema za izradu bakar-10%kalaj-nano ZrO₂ kompozita, primenom tehnike rastopa. U osnovnu matricu bakar-kalaj (Cu-Sn) se uvode ZrO₂ nanočestice od 4, 8 i 12 % tež. Ispitivanje mikrostrukture je izvedeno metodama SEM, EDS, i XRD. Mehaničke karakteristike Cu-10%Sn-4, 8, 12 % tež. nano ZrO₂ kompozita su izmerene shodno ASTM standardima. Skening elektronskom mikroskopijom otkriva se uniformna raspodela nano ZrO₂ unutar matrice bakar-kalaj amalgama. Istraživanja EDX potvrđuju prisustvo Zr i O u nano-ZrO₂ izgrađenom kompozitu, a izvođenjem XRD otkrivaju se faze Cu, Sn, i ZrO₂. Primećuje se porast tvrdoće, napona tečenja kod legure Cu-Sn, sa porastom sadržaja od 4, 8 i 12 %tež. nano ZrO₂. Izduženje nano kompozita opada sa dodavanjem čestica oksida. Fraktografija uzoraka za zatezanje je izvedena korišćenjem SEM mikrosnimaka, radi dobijanja uvida u razvoj loma komponenata.

Metal matrix composites are a unique combination of metallic alloys such as aluminium (Al), copper (Cu), zinc (Zn), magnesium (Mg), and titanium (Ti) that is reinforced with mostly ceramic particulates such as boron carbide, silicon carbide, alumina etc., to obtain better properties as associated to conventional monolithic materials, /5, 6/.

Amongst any of further normally utilized metals, copper is one portrayed by the best conductivity and confrontation to corrosion which clarifies why it is generally picked in the main case for metal material. Then again, having exceptionally lower properties, it has to be fortified by earthenware

particles, for example, which is one of the greatest consistent methods of strengthening copper based metallic matrix composites. Copper and its alloys are largely used as a material for bearings, /7/.

Zirconium oxide (ZrO₂) is a superior reinforcement substantially due to its great hardness and strength, good impact and wear resistance, with higher melting point, good chemical stability. The graphite reinforcement is a solid lubricant that reduces the wear of copper matrix with very good electrical conductivity when fabricated with copper, /8/.

Generally for bearing applications, most commonly used materials are copper, zinc, and aluminium alloys. Instead of using copper alone as a bearing material, most of the commercial industries are utilizing copper zinc alloy and copper tin alloys as materials for several applications. In the present work it is intended also to develop the copper zinc alloy and copper tin alloy based nano metal composites. The CuZn alloys (i.e. brasses) consist of a series of alloys with a copper content of 90, 80, 72, 67, 63 and 60 % (i.e. 10-40 % of Zn). The first two alloys possessing extremely good formability are mainly used to produce decorative artifacts. The rest of the alloys are known as brass. The CuSn alloy (tin bronze) has been used for a very long time. The Bronze Age (about 3000 years BC) is named after this alloy. It has been used by mankind to make utensils and decorative artifacts. However, it should be noted that CuSn alloys used in the industry have Sn content below 40 %.

The effective creation, applications, and properties of MMCs are to a great extent dependent upon the properties of constituents. The construction and conduct of the interface locale in MMCs are at the focal point of a significant part of principal research examinations. A few analysts created the different Al Cu, Zn and Mg combination composites by adding SiC, Al₂O₃, B₄C, and graphite particles, utilizing semisolid state and furthermore, by powder metallurgy (PM), /9/.

Stir projecting technique offers a few benefits, yet at the same time there are confusions in growing high quality particulate built-up MMCs, /10/. The genuine trouble is to achieve an extraordinary connection between Cu network mix and support, to restrict/avoid interfacial reaction between system compound and stronghold, and to improve wettability of fortress in grid material. One of the normal practices to enhance wettability of copper melt is through addition of small amounts of responsive metals as Mg, Ti, and so on. Additionally, wettability can be enhanced by utilizing metallic covered fortifications as graphite, TiO₂, Al₂O₃, and SiC /11, 12/. Further, coating of fortifications prompts moderate concoction collaboration among them and upgrades the quality at the interface, prompting in general enhancement in mechanical properties. Further, previous investigations reveal that only a very few studies have been made on the use of ZrO₂ as reinforcement to synthesize copper alloy with ZrO₂ composites by liquid melt technique. Prepared copper alloy with zirconium oxide composites is then subjected to evaluation of physical, mechanical, and wear.

In the present study, Cu-10%Sn alloy composites are fabricated by stir casting process. Nano ZrO₂ is used as the reinforcement. The 4, 8 and 12 wt. % of ceramics reinforce-

ments are used to fabricate the copper and ZrO₂ composites. These are tested for mechanical properties, as hardness, compressive strength, ultimate tensile- and yield strength, and percentage elongation, as per ASTM standards.

EXPERIMENTAL STUDY

Materials and composite preparation

The Cu-Sn-nano ZrO₂ composites fabricated in this study contain 4, 8, and 12 wt. % of ceramic nano ZrO₂. The density of Cu-Sn alloy is 8.76 g/cm³, and the density of ZrO₂ is 5.68 g/cm³. The density of composites decreases with addition of nano ZrO₂ particles. The chemical composition of copper-tin alloy is shown in Table 1. Figure 1 shows a SEM micrograph of 500 nm ZrO₂ particles, and Table 2 shows the various properties of ZrO₂.

Table 1. The chemistry of Cu-Sn alloy.

Elements	Content wt. %
Cu	89.40
Sn	9.98
other	0.62

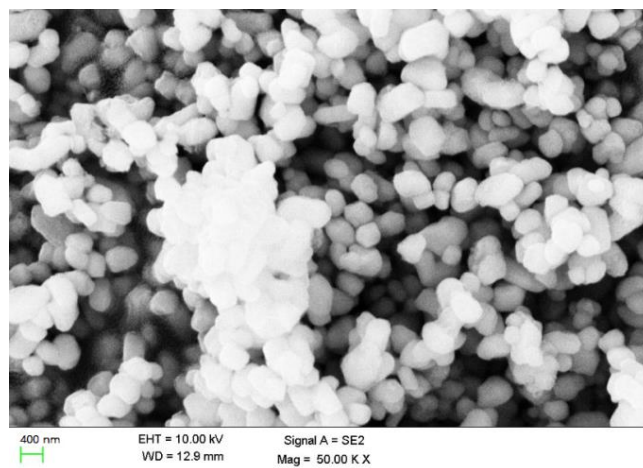


Figure 1. SEM micrograph of nano ZrO₂ particles.

Table 2. Properties of ZrO₂ particles.

Properties	ZrO ₂
Melting point (°C)	2715
Hardness (BHN)	1300
Density (g/cm ³)	5.68
CTE (10 ⁻⁶ °C)	11.6
Poisson's ratio	0.32
Colour	white

The method embraced for producing Cu 10% Sn and 4 wt. % of nano ZrO₂ composites is the liquid metallurgy strategy by stir procedure. Pre-decided loads of Cu10% Sn amalgam metal ingots are placed in the electric furnace and warmed up to liquid metal stage. Ordinarily, Cu-Sn compound begins dissolving at 1080 °C. However, the liquid metal is warmed up to 1150 °C. To quantify the dissolving and superheating temperatures, fitting thermocouples that depend on the temperature range are utilized, and these temperatures are recorded. The superheated liquid metal in the cauldron is degassed by utilizing hexachloroethane (C₂Cl₆) for around 3 minutes. Fan type steel rotor fixed on a shaft stirrer is covered with Zr clay material utilized for

blending the liquid metal. The stirrer is drenched in liquid metal; about 60 % of profundity in the cauldron, and by turning the stirrer at a speed of around 300 rpm, the liquid metal is unsettled to a degree of vortex creation. While blending the liquid metal, next to each other nano ZrO₂ particulates comparable to 4 % by weight of charged Cu-Sn compound, are likewise to be preheated in a different heater up to 500 °C, and it is emptied gradually into liquid metal vortex in stages. At that point, the liquid metal combination of CuSn amalgam lattice and ZrO₂ composites is poured in cast iron moulds of different measurements, in this manner delivering the Cu10%Sn with 4 wt. % of ZrO₂ nano composites. The same technique is embraced for delivering Cu 10% Sn with 8 wt. % of ZrO₂, and Cu10%Sn with 12 wt. % of ZrO₂. In Fig. 2 is the cast iron die used for manufacturing the composites.



Figure 2. Cast iron die.

Testing of nano composites

Using SEM equipment, microstructural studies are conducted. Test samples 5 mm thickness are used to capture the microstructure. Keller's reagent is used to clean the samples. Hardness of as cast Cu-Sn-ZrO₂ combination composites are facilitated to find the impact of nano scale ZrO₂ particles in the framework material according to ASTM E 10 standard /13/. The hardness test is done by Brinell hardness machine under 250 kg load with 5 mm ball indenter for a period of 30 seconds.

Specimens prepared as per ASTM E8 /14/ for tension test are subjected to uni-axial loading. The round specimen is fabricated to gauge diameter of 9 mm keeping gauge length of 45 mm. Figure 3 shows the tensile test specimen used in the work. The specimen is subjected to tensile test under Instron servo-hydraulic machine with a cross head speed set to 0.28 mm/min. Consequences of nano particles on the tensile behaviour of CuSn alloy composites are plotted. Further, percentage elongation, ultimate tensile- and yield strength values are recorded from the graphs and comparison is made. Similarly, the compression test is done by using the UTM and Fig. 4 shows the compression test specimen as per ASTM E9, /15/.



Figure 3. Tensile test specimen.

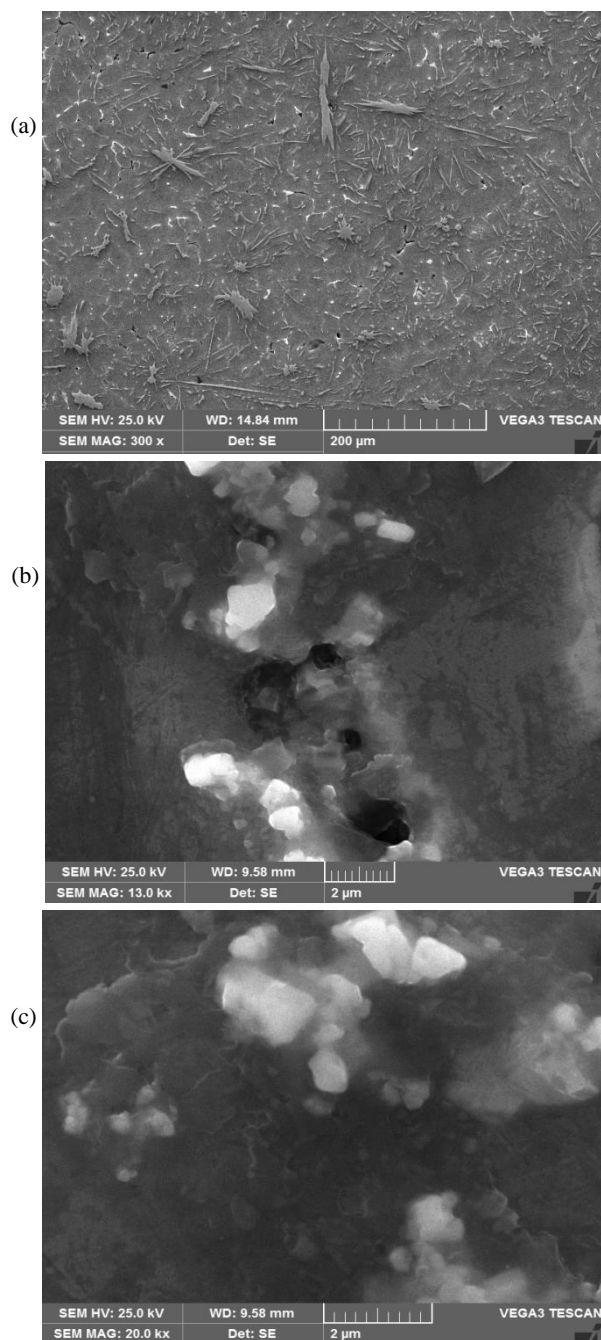


Figure 4. Compression test specimen.

RESULTS AND DISCUSSION

Microstructural analysis

Figure 5a-d shows SEM micrographs of Cu10% Sn alloy and nano ZrO₂ reinforced composites. Figure 5a shows the SEM of as-cast Cu10% Sn alloy. Figure 5b-d show SEM images of Cu10% Sn-4 wt. % ZrO₂, Cu10% Sn-8 wt.% ZrO₂ and Cu10% Sn with 12 wt.% ZrO₂ composites, in respect. It confirms that most of nano ZrO₂ particles are mixed uniformly in Cu10%Sn alloy. Further, these figures disclose the regularity of the prepared composites. The micrographs also clearly indicate the increased reinforcement contents in Cu10%Sn alloy composites.



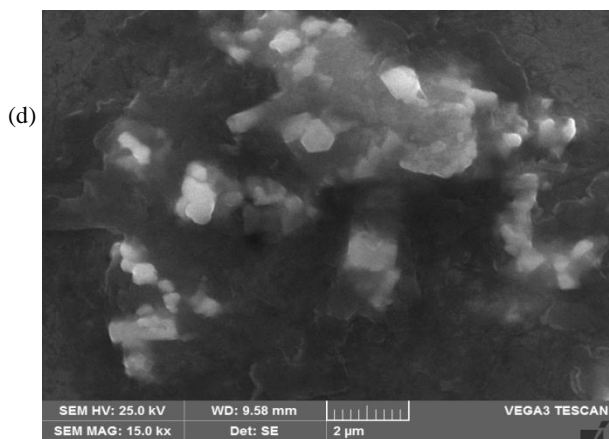


Figure 5. SEMs of: a) Cu10%Sn alloy; b) Cu10%Sn-4% ZrO₂; c) Cu10%Sn-8% ZrO₂; d) Cu10%Sn-12% ZrO₂ composites.

The SEM micrographs disclose that the distribution of nano ZrO₂ reinforcement particles of different wt.% is almost uniform throughout the Cu10%Sn matrix, as revealed in Fig. 5b-d above. It is also revealed that there are no discontinuities, voids, and cold shuts. Good interfacial bonding of nano ZrO₂ reinforcement particles and Cu10%Sn alloy matrix is observed. From the above SEM explanation, a uniform distribution of reinforcement particles is evident, with no defects in castings, and good interfacial bonding in the Cu 10%Sn-ZrO₂ particulate composite, thereby increasing the overall strength of the MMC, and its substantial effect on both mechanical and tribological properties, /16, 17/.

The EDS technique is adopted for elemental analysis of Cu10%Sn alloy, and Cu10%Sn and ZrO₂ reinforced composites. Compositions of the composites are shown in Fig. 6a-d.

Figure 6a shows the EDS spectrograph of as-cast Cu10%Sn alloy. The spectrum confirms the presence of Cu as the highest element followed by Sn as other alloying element. In Fig. 6b-d are shown EDS of Cu10%Sn with 4 wt.% of ZrO₂, Cu10%Sn with 8 wt.% of ZrO₂, and Cu10%Sn with 12 wt.% of ZrO₂. It is evident that the presence of ZrO₂ in the Cu10%Sn alloy is confirmed by elements Zr and O in the obtained spectrographs.

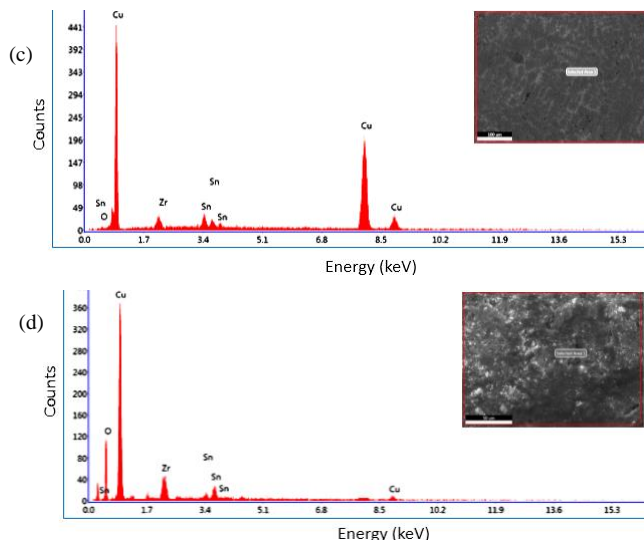
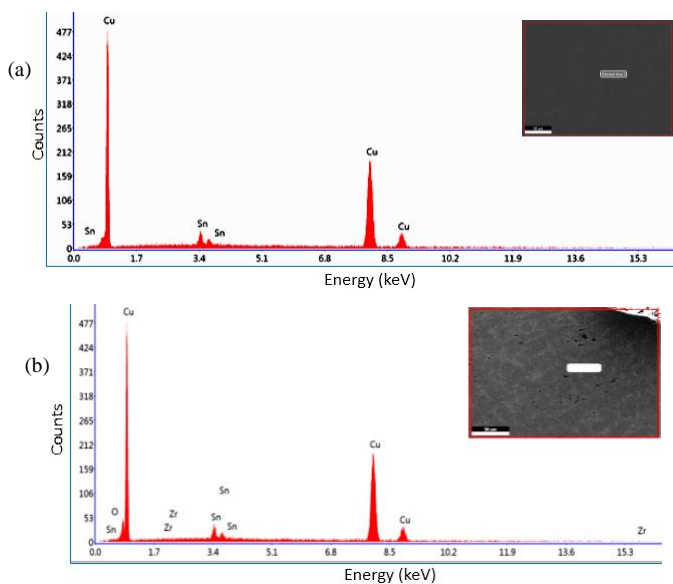
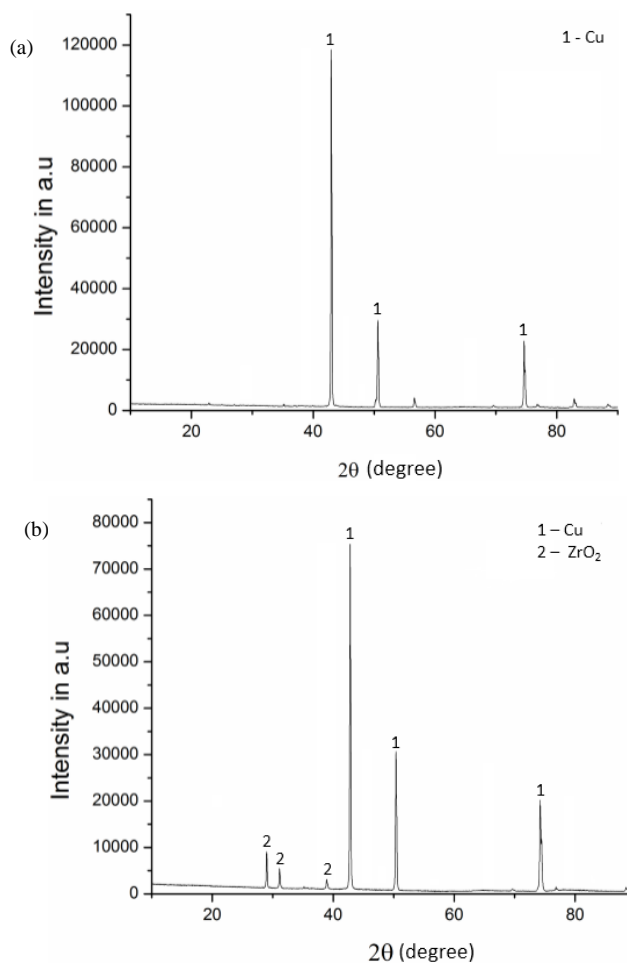


Figure 6. EDSs of: a) Cu10%Sn alloy; b) Cu10%Sn with 4% ZrO₂; c) Cu10%Sn with 8% ZrO₂; d) Cu10%Sn with 12% ZrO₂.

All spectrographs contain Zr and O elements along with Cu and Sn, in Fig. 6b-d, confirming the presence of nano ZrO₂ in the CuSn-based alloy matrix.

Figure 7a shows the XRD pattern for as-cast Cu10%Sn alloy to verify its quality and standard XRD pattern. It is visible that peak X-ray intensities are higher at 43°, 51° and 75°, indicating the presence of Cu phase.



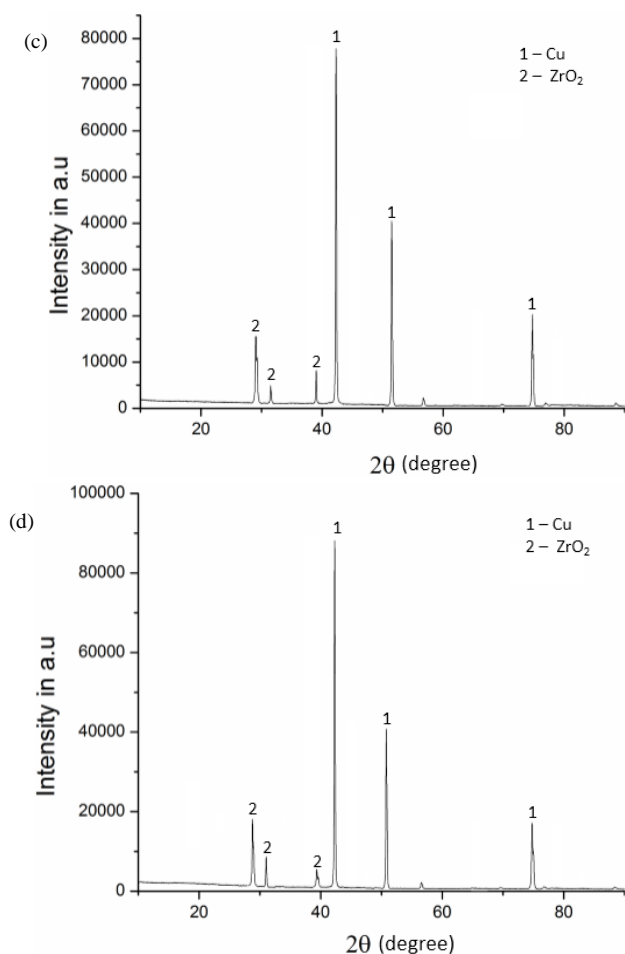


Figure 7. XRD patterns of: a) as-cast Cu10%Sn alloy; b) Cu10%Sn with 4% ZrO₂; c) Cu10%Sn with 8% ZrO₂; d) Cu10%Sn with 12% ZrO₂ composites.

Figure 7b-d shows XRD patterns in respect for Cu10% Sn with 4, 8, and 12 wt.% of ZrO₂ reinforced composites to verify its quality and standard pattern. In Fig. 7b-d the peaks are observed for different phases of Cu, Sn, and ZrO₂. It is visible that peaks are higher at 43°, 51°, and 75°, demonstrating the presence of Cu phase, and similarly the peaks at 29°, 31° and 39° are indicating the presence of ZrO₂ phases.

Density measurements

Figure 8 compares theoretical and experimental densities of as-cast Cu10 wt.% Sn alloy, and Cu10 wt.% Sn with 4, 8, and 12 wt.% of ZrO₂ composites, in respect. Cu10 wt.% Sn alloy has a density of 8.76 g/cm³, ZrO₂ has a density of 5.68 g/cm³, and when Cu10 wt.% Sn alloy is reinforced with 4 wt.% of nano ZrO₂, the overall density of composite becomes less as ZrO₂ density is lesser than the CuSn alloy, and the density of Cu10 wt.% Sn with 4 wt.% of ZrO₂ is 8.57 g/cm³. Similarly, when 8 and 12 wt.% ZrO₂ particles are reinforced within CuSn alloy, the overall density of the composite tends to become lesser than that of previous/base Cu-Sn alloy. Further, it can be observed that experimental densities are lesser than the theoretical. Further, from Fig. 8 the experimental densities are nearer to theoretical densities, which indicate the quality of the prepared specimens.

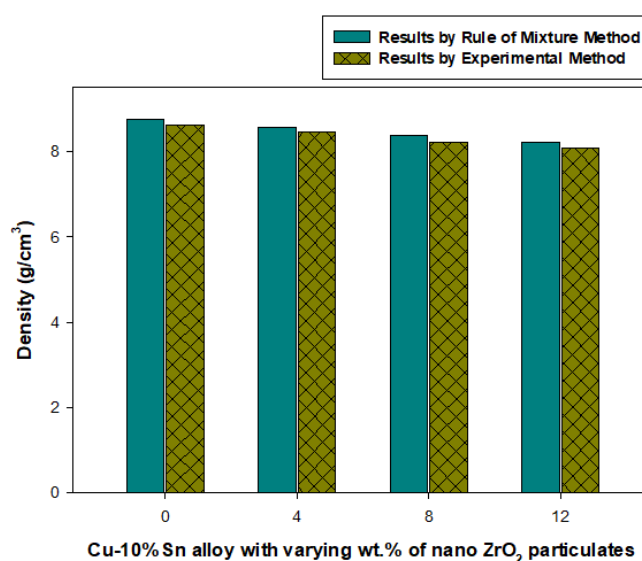


Figure 8. Theoretical and experimental densities of Cu10 wt.% Sn alloy with nano ZrO₂ reinforced composites.

Hardness measurements

Figure 9 shows the effect of nano ZrO₂ particles addition on the hardness of Cu 10 wt.% Sn alloy. It is noted that as the wt.% of nano ZrO₂ particles increases in the Cu10 wt.% Sn alloy, there is increase in hardness. The hardness of as-cast Cu10 wt.% Sn alloy is 69.1 BHN. Further, the hardness of the Cu10 wt.% Sn with 4, 8, and 12 wt.% ZrO₂ composites is respectively 75.4, 82.9, and 90.8 BHN. The trend of increase in hardness is due to the hardness of ZrO₂ particles, which being uniformly dispersed add to the hardness of the composite, since they act as barriers to the progress of dislocations within the matrix [18]. The observations and obtained results are consistent with the results of other researchers. This may be mainly due to the good bonding between base and fortification.

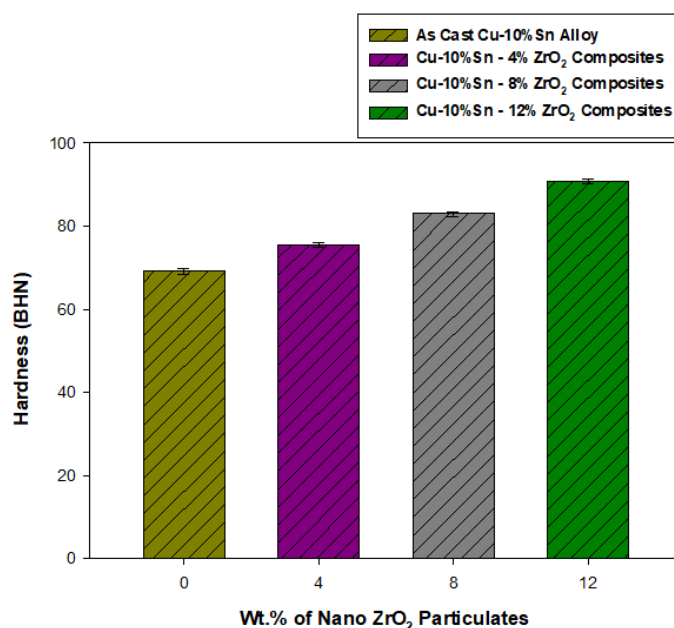


Figure 9. Hardness of Cu10 wt.% Sn alloy with nano ZrO₂ composites.

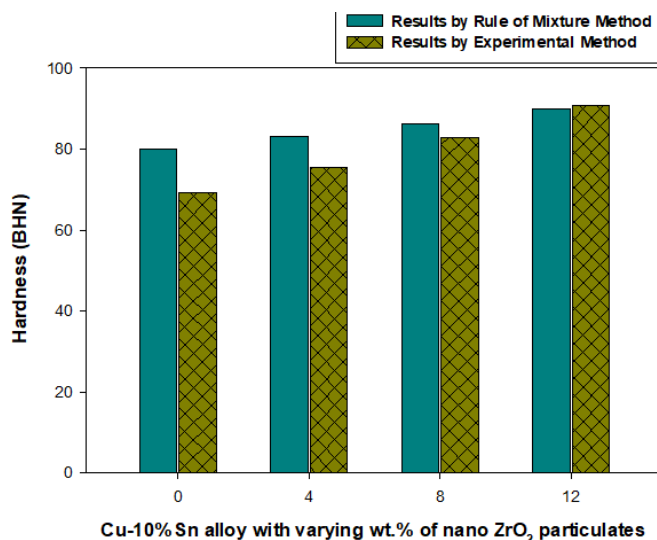


Figure 10. Theoretical and experimental hardness of Cu10 wt.% Sn alloy with nano ZrO₂ reinforced composites.

Comparison of theoretical and experimental hardness is made in Fig. 10. Theoretical hardness of Cu10% Sn with 12 wt.% ZrO₂ composite is 89.97 BHN, which is determined by using the rule of mixture method. Further, experimental hardness of Cu10% Sn -12 wt.% ZrO₂ composite is 90.8 BHN. Adding the nano ZrO₂ enhances the hardness of Cu-Sn matrix alloy. As the wt.% of nano ZrO₂ particles increases from 4 to 12 wt.%, there is an increase in hardness of the Cu-Sn alloy. The increasing trend of hardness is observed both in the theoretical and experimental values. Further, from Fig. 10, both experimental and theoretical hardness values are almost in the similar range.

Tensile properties

Figure 11 shows the experimental tensile strength of Cu 10 wt.% Sn alloys, with 4, 8, and 12 wt.% ZrO₂ composites, in respect. The UTS is increases with increasing nano ZrO₂ content. The ZrO₂ particle in the matrix alloy provides the protection to the softer matrix. The experimental UTS of as cast Cu10 wt.% Sn alloy is 272.4 MPa. Further, as weight

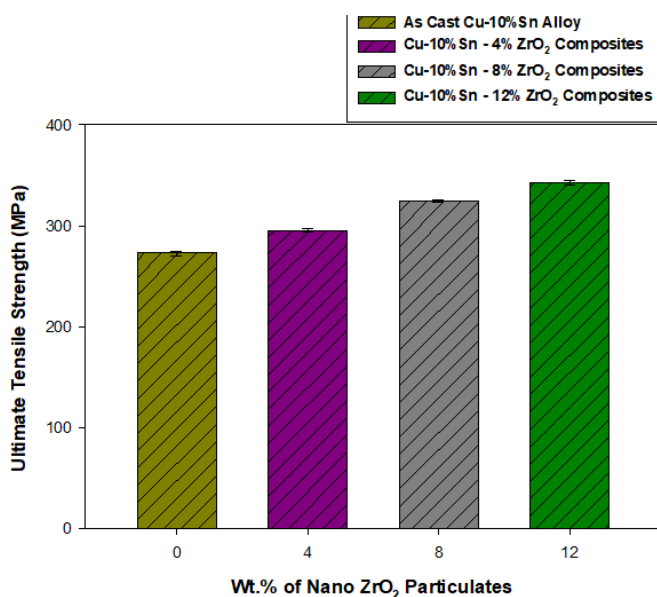


Figure 11. UTS of Cu10 wt.% Sn alloy with nano ZrO₂ composites.

percentage of nano ZrO₂ particulates increases from 4 to 12 wt.% in steps of 4 wt.%, there is an increase in UTS values. It is observed that in Cu10 wt.% Sn with 4, 8, and 12 wt.% ZrO₂ composites, the UTS is 294.6, 324.5 and 341.6 MPa, in respect. Improvement of the experimental UTS of as-cast Cu10 wt.% Sn alloy is 25.4 % after incorporating 12 wt.% nano ZrO₂ particulates.

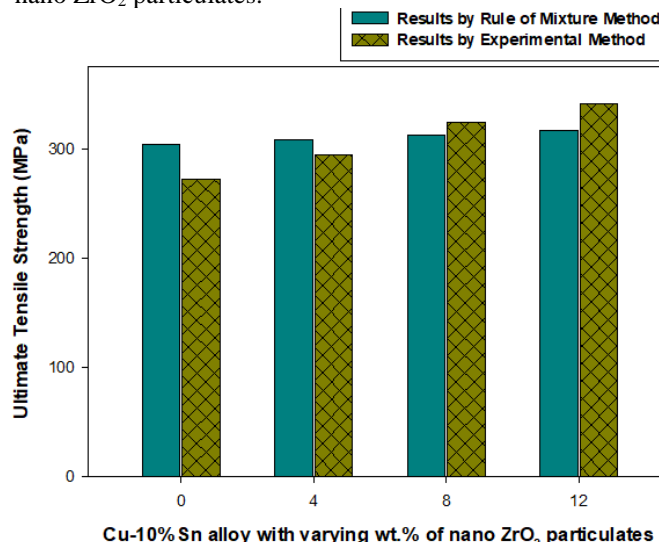


Figure 12. Theoretical and experimental UTS of Cu10 wt.% Sn alloy with nano ZrO₂ reinforced composites.

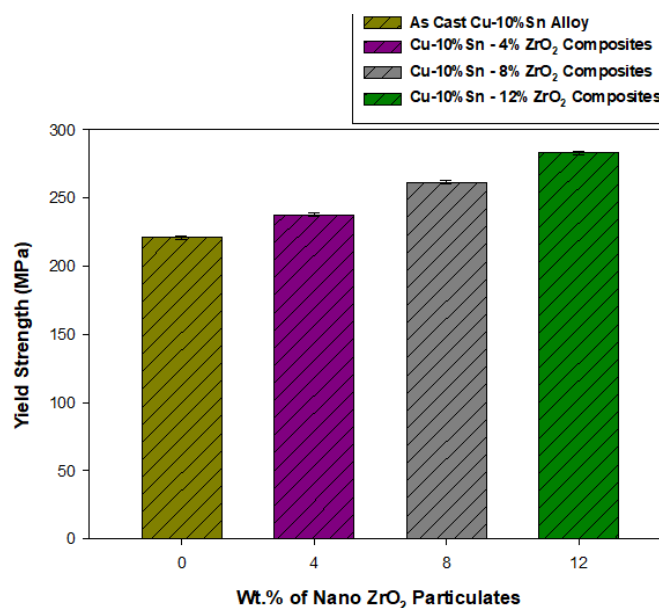


Figure 13. YS of Cu10 wt.% Sn alloy with nano ZrO₂ composites.

Figure 12 shows the comparison between theoretical and experimental UTS of Cu10 wt.% Sn alloy, with 4, 8, and 12 wt.% ZrO₂ composites, respectfully. The theoretical UTS of CuSn alloy and its varying wt.% of ZrO₂ nano particulates reinforced composites are estimated by using the rule of mixture. Further, these theoretical UTS values are compared with experimental UTS values obtained by conducting the tensile test as per ASTM standard. From Fig. 12 as the wt. % of nano ZrO₂ particulates rises from 4 to 12 wt.%, there is an increase of UTS in the cases of both theoretical and experimental values. Theoretical and experimental UTS results are almost travelling parallel in Fig. 12. Theoretical

and experimental UTS of Cu10 wt.% Sn with 12 wt.% ZrO₂ composite are 316.81 and 341.6 MPa, respectively.

Figure 13 shows the yield strength (YS) of CuSn alloy with 4, 8, and 12 wt.% of nano ZrO₂ reinforced composites. It is evident that as wt.% of ZrO₂ content increases from 4 to 12 wt.%, there is an increase in YS of CuSn alloy. The yield strengths of CuSn alloy, and with 4, 8, and 12 wt.% of ZrO₂ are 221.1, 237.1, 260.9, and 283.3 MPa, respectively. The addition of ZrO₂ particles to the CuSn alloy matrix improves the YS by acting as a barrier for plastic deformation.

Figure 14 denotes the percent elongation of as-cast CuSn alloy, CuSn alloy with 4, 8, and 12 wt.% of nano size ZrO₂ particulate composites, as a result in tensile testing. The percentage elongation of as-cast CuSn alloy decreases after the addition ZrO₂ particulates; it further decreases as the % of reinforcement increases in the CuSn alloy. The elongation of CuSn alloy is 14.9 %, and after adding 12 wt.% of ZrO₂ particles, it decreases to 12.2 %.

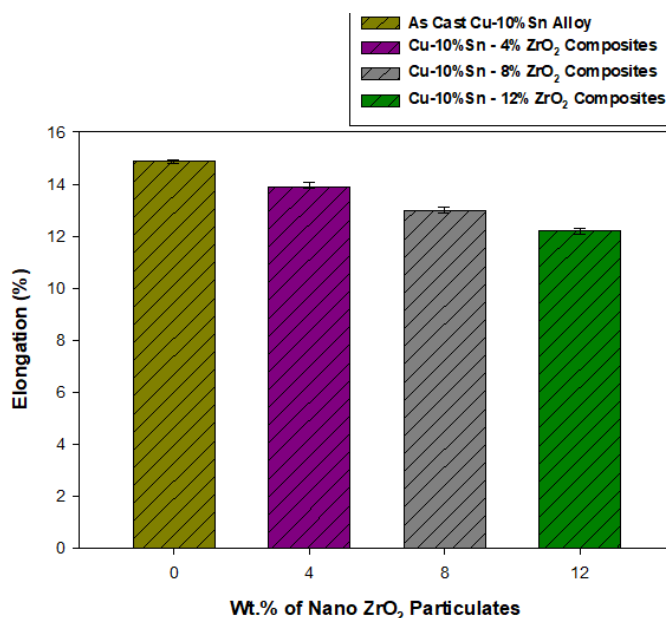


Figure 14. Percentage elongation of Cu10 wt.% Sn alloy with nano ZrO₂ composites.

Compressive strength

Figure 15 shows the compressive strength of CuSn alloy and 4, 8, and 12 wt.% of nano ZrO₂ composites. It is evident that as the percentage of ZrO₂ increases from 4 to 12 wt.%, there is an increase in compressive strength of the CuSn alloy. The experimental compressive strength of CuSn alloy is 465.1 MPa, and in the case of CuSn alloy with 4, 8, and 12 wt.% of ZrO₂, it is 495.6, 539.2, and 565.2 MPa, in respect.

Comparison of theoretical and experimental compressive strength is made in Fig. 16. The theoretical compressive strength of Cu10% Sn -12 wt.% of ZrO₂ composite is 545.68 MPa, determined by using the rule of mixture. Further, experimental compressive strength of Cu10% Sn with 12 wt.% of ZrO₂ composite is 565.2 MPa. The addition of nano ZrO₂ particles enhances the strength of the Cu matrix alloy. As wt.% of nano ZrO₂ increases from 4 to 12 wt.%, there is an increase in compressive strength of the Cu-Zn alloy.

The increasing trend of compressive strength is observed in both theoretical and experimental values. Further, from Fig. 16, both experimental and theoretical values are almost in the similar range.

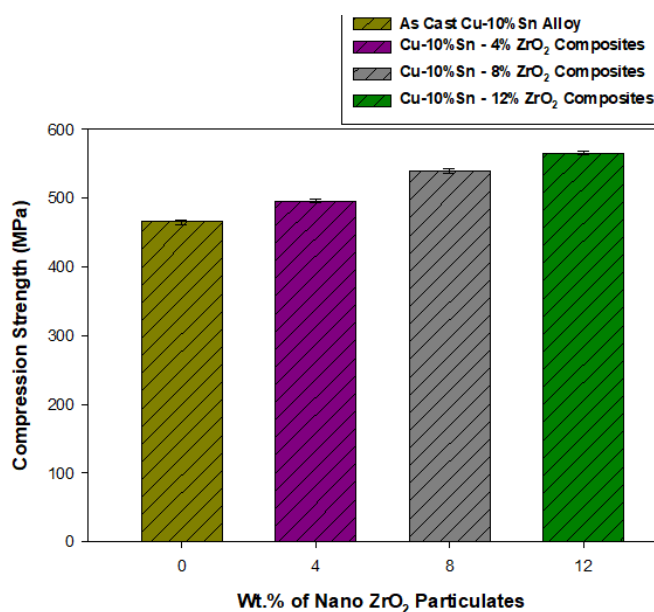


Figure 15. Compressive strength of Cu10 wt.% Sn alloy with nano ZrO₂ composites.

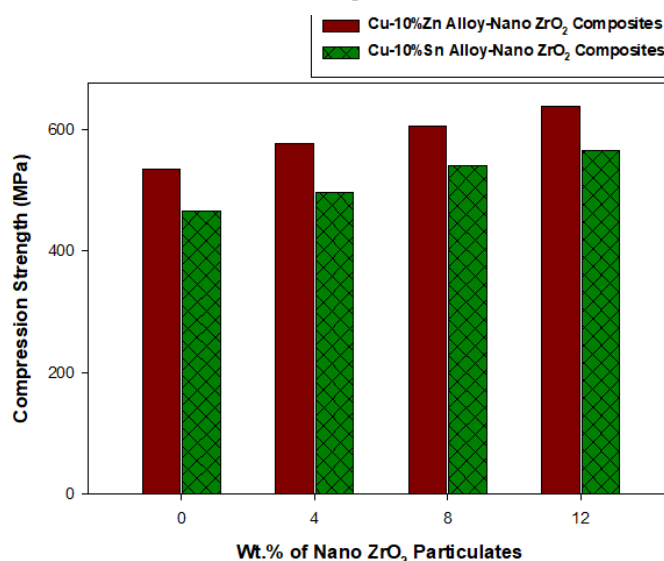


Figure 16. Compressive strength comparison for Cu10 wt.% Zn and Cu10 wt.% Sn alloys with nano ZrO₂ reinforced composite.

Fractography

Fractured surfaces of the alloys and their composites are studied to identify the cause of failure of the fabricated composite materials. SEM images of tensile fractured surfaces are shown in Fig. 17a-d.

SEM examination of as-cast CuSn alloy shows a dimpled fracture surface, leading to the evidence of ductile fracture, whereas SEM examination for reinforced CuSn-4, 8, and 12 wt.% nano ZrO₂ material shows irregular circulation of large dimples connected by pieces of smaller dimples, representing a pattern resultant from ductile void growth coalescence, but a higher percentage of ZrO₂ particulate reinforced composites

shows brittle fracture failure /19, 20/. Hence, it is likely that the properties of ZrO₂ have significant impact on composite mechanical properties.

CONCLUSION

The copper-tin alloy with 4 to 12 wt.% of nano ZrO₂ particulate composites has been successfully fabricated by stir casting route. The SEM microphotos reveal an even dissemination of nano ZrO₂ particles in the Cu10 wt.% Sn alloy composites. EDS and XRD analysis reveal the presence of nano ZrO₂ particles in Cu10 wt.% Sn alloy composites in the form of Zr and O elements. Theoretical and experimental densities of CuSn with ZrO₂ composites decrease as the wt.% of reinforcement increases from 4 to 12 wt.%. The hardness, tensile, and compressive strengths of Cu10 wt.% Sn alloy with 4 to 12 wt.% of ZrO₂ composites increases with the addition of ZrO₂ particles. Percentage elongation of the CuSn alloys decreases with the addition of nano ZrO₂ particles. It decreases further as the wt.% of the reinforcement increases from 4 to 12 wt.%. Fractography analysis indicates various fracture mechanisms in CuSn alloy matrices with 4 to 12 wt.% of nano ZrO₂ composites.

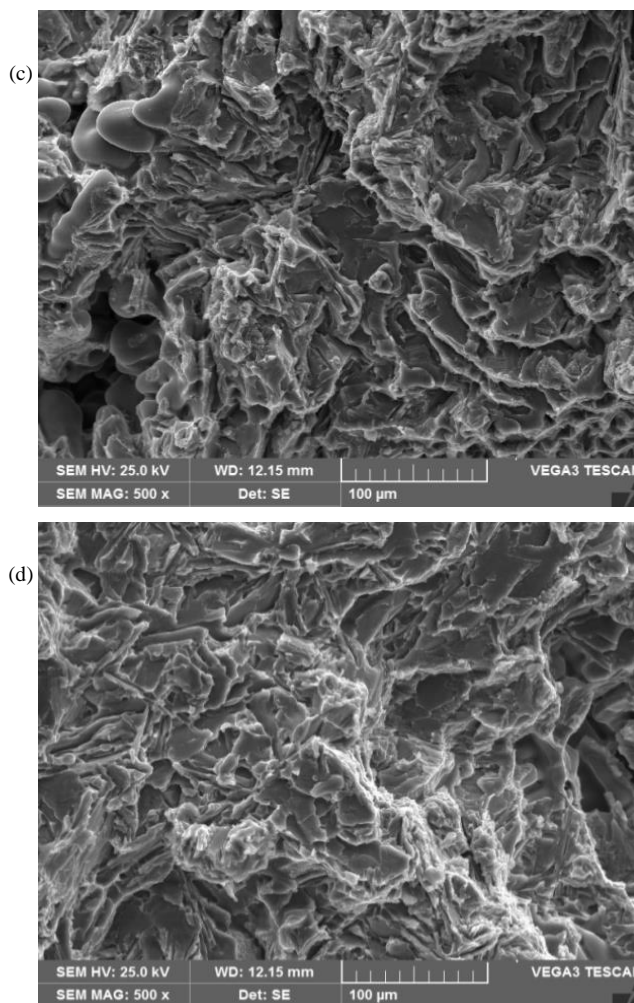
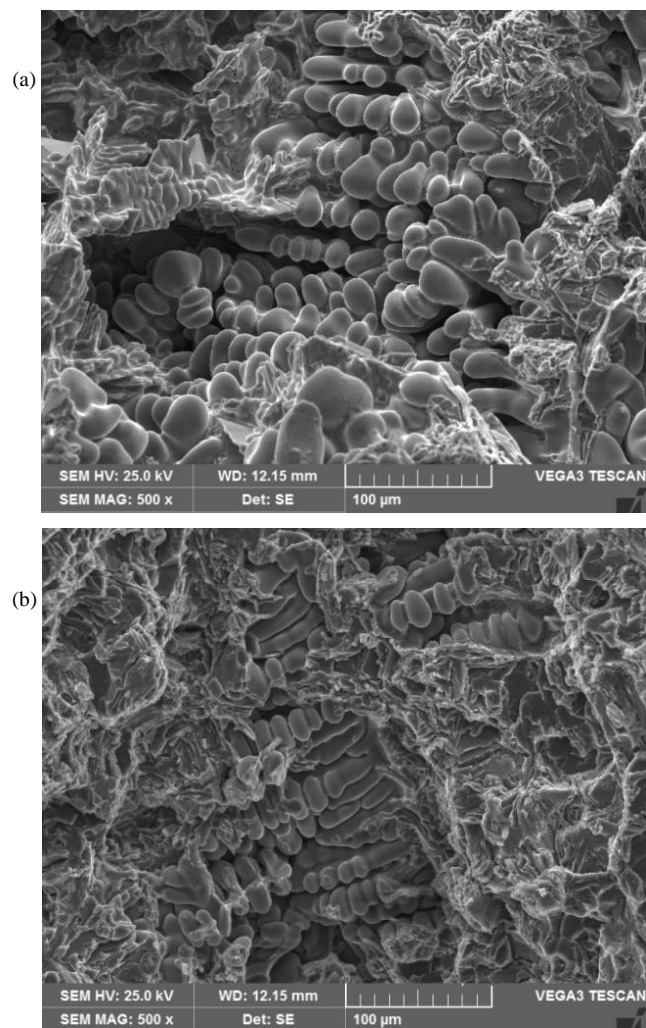


Figure 17. SEMs of tensile fractured surfaces: a) CuSn alloy; b) CuSn-4 wt.% ZrO₂; c) CuSn-8 wt.% ZrO₂; d) CuSn-12 wt.% ZrO₂ composites.

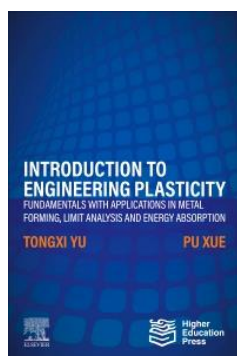
REFERENCES

1. Nagaral, M., Kalgudi, S., Auradi, V., Kori, S.A. (2018), *Mechanical characterization of ceramic nano B₄C- Al2618 alloy composites synthesized by semi solid state processing*, Trans. Indian Cer. Soc. 77(3): 146-149. doi: 10.1080/0371750X.2018.1506363
2. Nagaral, M., Shivananda, B.K., Auradi, V., et al. (2017), *Mechanical behavior of Al6061-Al₂O₃ and Al6061-graphite composites*, Mater. Today: Proc. 4(10): 10978-10986. doi: 10.1016/j.matpr.2017.08.055
3. Jadhav, P., Sridhar, B.R., Nagaral, M., et al. (2018), *A comparative study on microstructure and mechanical properties of A356-B₄C and A356-graphite composites*, Int. J Mech. Prod. Eng. Res. Devel. 8(2): 273-282.
4. Nagaral, M., Auradi, V., Kori, S.A., Hiremath, V. (2019), *Investigations on mechanical and wear behavior of nano Al₂O₃ particulates reinforced AA7475 alloy composites*, J Mech. Eng. Sci. 13(1): 4623-4635. doi: 10.15282/jmes.13.1.2019.19.0389
5. Harti, J.I., Prasad, T.B., Nagaral, M., et al. (2017), *Microstructure and dry sliding wear behaviour of Al2219-TiC composites*, Mater. Today: Proc. 4(10): 11004-11009. doi: 10.1016/j.matpr.2017.08.058
6. Mazahery, A., Ostad Shabani, M. (2013), *Microstructural and abrasive wear properties of SiC reinforced aluminum-based composite produced by compocasting*, Trans. Nonferr. Met. Soc. China, 23(7): 1905-1914. doi: 10.1016/S1003-6326(13)62676-X

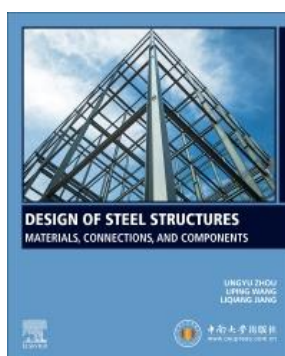
7. Nayak, P.H., Srinivas, H.K., Nagaral, M., Auradi, V. (2019), *Characterization and tensile fractography of nano ZrO₂ reinforced copper-zinc alloy composites*, *Frattura ed Integ. Strutturale*, 13 (48): 370-376. doi: 10.3221/IGF-ESIS.48.35
8. Nagaral, M., Hiremath, V., Auradi, V., Kori, S.A. (2018), *Influence of two-stage stir casting process on mechanical characterization and wear behavior of AA2014-ZrO₂ nano-composites*, *Trans. Ind. Inst. Met.* 71: 2845-2850. doi: 10.1007/s12666-018-1441-6
9. Kumar, L., Nasimul Alam, S., Kumar Sahoo, S., Teja, M.B.K. (2018), *Mechanical properties of Cu-MWCNT composites developed by powder metallurgy route*, *Mater. Today: Proc.* 5(9): 19883-19892. doi: 10.1016/j.matpr.2018.06.353
10. Nagaral, M., Shivananda, B.K., Jayachandran, et al. (2016), *Effect of SiC and graphite particulates addition on wear behaviour of Al2219 alloy hybrid composites*, *IOP Conf. Ser.: Mater. Sci. Eng.* 149: 012108. doi: 10.1088/1757-899X/149/1/012108
11. Bharath, V., Nagaral, M., Auradi, V., Kori, S.A. (2014), *Studies on dry sliding wear characteristics of ceramic Al₂O₃ particulate reinforced 6061Al matrix composites*, *Adv. Mater. Res.* 984-985: 319-325. doi: 10.4028/www.scientific.net/AMR.984-985.319
12. Mallikarjuna, H.M., Kashyap, K.T., Koppad, P.G., et al. (2016), *Microstructure and dry sliding wear behavior of Cu-Sn alloy reinforced with multiwalled carbon nanotubes*, *Trans. Nonferr. Met. Soc. China*, 26(7): 1755-1764. doi: 10.1016/S1003-6326(16)64269-3
13. Ezatpour, H.R., Torabi-Parizi, M., Sajjadi, S.A. (2013), *Microstructure and mechanical properties of extruded Al/Al₂O₃ composites fabricated by stir-casting process*, *Trans. Nonferr. Met. Soc. China*, 23(5): 1262-1268. doi: 10.1016/S1003-6326(13)62591-1
14. Fazil, N., Venkataraman, V., Nagaral, M. (2020), *Mechanical characterization and wear behavior of aerospace alloy AA2124 and micro B₄C reinforced metal composites*, *J Met., Mater. Miner.* 30(4): 97-105. doi: 10.14456/jmmm.2020.57
15. Shashidhar, S., Kumar, P.V., Shivanand, H.K., Nagaral, M. (2018), *Processing, microstructure, density and compression behaviour of nano B₄C particulates reinforced Al2219 alloy composites*, *Int. J. Adv. Technol. Eng. Expl.* 5(46): 350-355. doi: 10.19101/IJATEE.2018.546015
16. Prasad, G.P., Chittappa, H.C., Nagaral, M., Auradi, V. (2020), *Influence of B₄C reinforcement particles with varying sizes on the tensile failure and fractography of LM29 alloy composites*, *J Fail. Anal. Prev.* 20(6): 2078-2086. doi: 10.1007/s11668-020-01021-6
17. Bharath, V., Ashita, D.H., Auradi, V., Nagaral, M. (2020), *Influence of variable particle size reinforcement on mechanical and wear properties of alumina reinforced 2014Al alloy particulate composite*, *FME Trans.* 48(4): 968-978. doi: 10.5937/fme2004968B
18. Bharath, V., Auradi, V., Nagaral, M., Bopanna, S.B. (2020), *Experimental investigations on mechanical and wear behaviour of 2014Al-Al₂O₃ composites*, *J Bio Tribo Corros.* 6: 45. doi: 10.1007/s40735-020-00341-2
19. Harti, J.I., Prasad, T.B., Nagaral, M., et al. (2021), *Microstructure, mechanical behavior and tensile fractography of 90-micron sized titanium carbide particles reinforced Al2219 alloy die cast metal composites*, *J Fail. Anal. Preven.* 21: 631-639. doi: 10.1007/s11668-020-01107-1
20. Kumar, R., Deshpande, R.G., Gopinath, B., et al. (2021), *Mechanical fractography and worn surface analysis of nanographite and ZrO₂-reinforced Al7075 alloy aerospace metal composites*, *J Fail. Anal. Preven.* 21: 525-536. doi: 10.1007/s11668-020-01092-5

© 2022 The Author. Structural Integrity and Life, Published by DIVK (The Society for Structural Integrity and Life 'Prof. Dr Stojan Sedmak') (<http://divk.inovacionicentar.rs/ivk/home.html>). This is an open access article distributed under the terms and conditions of the [Creative Commons Attribution-NonCommercial-NoDerivatives 4.0 International License](https://creativecommons.org/licenses/by-nc-nd/4.0/)

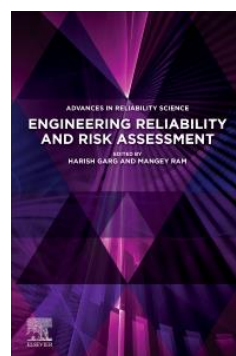
New Elsevier Book Titles – Woodhead Publishing – Academic Press – Butterworth-Heinemann – ...



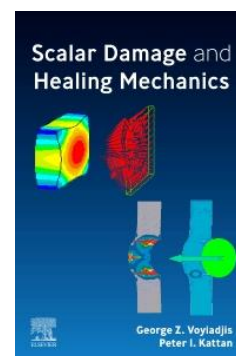
Introduction to Engineering Plasticity
Fundamentals with Applications in Metal Forming, Limit Analysis and Energy Absorption, 1st Edition
Tongxi Yu, Pu Xue
Elsevier, June 2022
ISBN: 9780323989817
EISBN: 9780323989824



Design of Steel Structures
Materials, Connections, and Components, 1st Edition
Lingyu Zhou, Liping Wang, Liqiang Jiang
Elsevier, August 2022
ISBN: 9780323916820
EISBN: 9780323916837



Engineering Reliability and Risk Assessment, 1st Edition
Harish Garg, Mangey Ram (Eds.)
Elsevier, September 2022
ISBN: 9780323919432
EISBN: 9780323913836



Scalar Damage and Healing Mechanics, 1st Edition
George Z. Voyiadjis, Peter I. Kattan
Elsevier, October 2022
ISBN: 9780128233399
EISBN: 9780128236178